Journal of Hazardous Materials 504 (2026) 141289

Contents lists available at ScienceDirect

Journal of Hazardous Materials

journal homepage: www.elsevier.com/locate/jhazmat

Dominant contribution of fossil fuel combustion to carbonaceous aerosol pollution in Delhi: Insights from radiocarbon and organic tracers

Zhenyu Wang [a,b], Deepchandra Srivastava [c], Mohammed S. Alam [c,d], Leigh R. Crilley [e], Louisa J. Kramer [c], Daniel J. Rooney [c], Supattarachai Saksakulkrai [c], Mukesh Khare [f], Philippa Ascough [d], Nicolas Bompard [g], Pauline Gulliver [g], Richard Shanks [g], Xiaomei Xu [h], James M. Cash [i], Chiara F. Di Marco [i], Ben Langford [i], Eiko Nemitz [i], Shivani [j], Ranu Gadi [j], Roy M. Harrison [c], William J. Bloss [c], Guoliang Shi [a,b,*], Zongbo Shi [c,**]

[a] Key Laboratory of Urban Air Particulate Pollution Prevention and Control of Ministry of Ecology and Environment, College of Environmental Science and Engineering, Nankai University, Tianjin 300350, China
[b] CMA-NKU Cooperative Laboratory for Atmospheric Environment-Health Research (CLAER), College of Environmental Science and Engineering, Nankai University, Tianjin 300350, China
[c] School of Geography Earth and Environment Sciences, University of Birmingham, Birmingham B15 2TT, UK
[d] School of Biosciences, Sutton Bonington, University of Nottingham, Loughborough LE12 5RD, UK
[e] Department of Chemistry, York University, Toronto, ON, Canada
[f] Department of Civil Engineering, Indian Institute of Technology Delhi, Hauz Khas, New Delhi 110016, India
[g] Scottish Universities Environmental Research Centre, East Kilbride G75 OQF, UK
[h] Earth System Science Department, University of California, IrvineCA92697USA
[i] UK Centre for Ecology and Hydrology, Penicuik, Midlothian EH26 0QB, UK
[j] Indira Gandhi Delhi Technical University for Women, Delhi 110006, India

HIGHLIGHTS

- Radiocarbon analysis was performed on carbonaceous aerosols from Delhi.
- Fossil fuel combustion was identified as the dominant source.
- Comparison of source contributions from different methods.
- The contribution from biomass burning was smaller than expected.

GRAPHICAL ABSTRACT

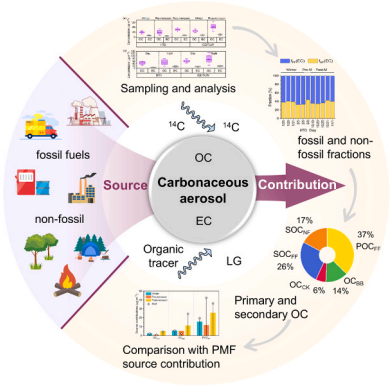

* Corresponding author at: Key Laboratory of Urban Air Particulate Pollution Prevention and Control of Ministry of Ecology and Environment, College of Environmental Science and Engineering, Nankai University, Tianjin 300350, China.
** Corresponding author.
E-mail addresses: nksgl@nankai.edu.cn (G. Shi), z.shi@bham.ac.uk (Z. Shi).

https://doi.org/10.1016/j.jhazmat.2026.141289
Received 23 October 2025; Received in revised form 19 January 2026; Accepted 27 January 2026
Available online 9 February 2026

ARTICLE INFO

Keywords:
Carbonaceous aerosols
Radiocarbon isotope
Source apportionment
Particulate matter

ABSTRACT

Delhi experiences some of the highest levels of fine particulate matter ($PM_{2.5}$) pollution among megacities worldwide. Here, we integrated radiocarbon (^{14}C) analysis with organic molecular tracers to quantify the sources of carbonaceous aerosols in Delhi. Through time-resolved seasonal and diurnal $PM_{2.5}$ sampling at two representative urban sites and using ^{14}C as an unambiguous tracer, we provide robust quantitative constraints on source contributions. We found that fossil fuel combustion is the dominant contributor, accounting for 62–65 % of organic carbon and 64–66 % of elemental carbon in $PM_{2.5}$. Crucially, primary organic carbon from fossil fuels (POC_{FF}) constituted the largest fraction of $PM_{2.5}$ organic carbon (31–44 %). Its contribution peaked in the post-monsoon season, driven mainly by traffic emissions and coal combustion. Secondary organic carbon from fossil sources (SOC_{FF}), biomass burning (OC_{BB}), and cooking emissions (OC_{CK}) contributed 21–29 %, 10–18 % and 3–7 % of $PM_{2.5}$ organic carbon, respectively. Furthermore, comparisons with Positive Matrix Factorization (PMF) results suggest that conventional methods may overestimate the biomass burning contribution, underscoring the value of the ^{14}C-based approach for accurate apportionment in this complex environment. This study underscores the critical need to reduce fossil fuel reliance and accelerate the shift toward clean energy infrastructure to effectively combat carbonaceous aerosol pollution in Delhi.

1. Introduction

Deteriorating air quality is a global concern [1–3]. Atmospheric fine particulate matter ($PM_{2.5}$), particularly carbonaceous aerosols, exerts significant impacts on climate and human and environmental health [4–8]. Carbonaceous aerosols are a major component of $PM_{2.5}$, accounting for approximately 40 % of the global total $PM_{2.5}$ mass [9], with regional contributions reaching up to 80 % [10, 11]. Typically, carbonaceous material can be classified into elemental carbon (EC) and organic carbon (OC) based on physicochemical properties [12]. EC originates predominantly primary emissions from fossil fuels or incomplete biomass burning [13], whereas OC derives from both primary emissions (POC) and secondary formation (SOC), the latter formed via photochemical oxidation of volatile organic compounds [14].

Frequent severe haze events have been plaguing air quality in India [15–19]. Recent studies estimate that air pollution caused ~1.24 million deaths in India in 2017 [1], rising sharply to 1.67 million by 2019 [20]. As one of the world's most polluted megacities, Delhi epitomizes this crisis. Studies show that from 2013 to 2021, the annual average $PM_{2.5}$ concentration in Delhi was 126 ± 77 $\mu g \cdot m^{-3}$, ranging from 17 to 581 $\mu g \cdot m^{-3}$ [21]. Notably, Delhi experiences an exceptionally high load of carbonaceous aerosols, typically accounting for 30–50 % of $PM_{2.5}$ mass, with total carbon (TC = OC + EC) concentrations often exceeding 50 $\mu g \cdot m^{-3}$ and peaking above 100 $\mu g \cdot m^{-3}$ during severe pollution episodes [15, 19, 22, 23]. An investigation into carbonaceous aerosols in $PM_{2.5}$ from an industrial area of Delhi in 2011 reported an annual average $PM_{2.5}$ concentration of 145.59 $\mu g \cdot m^{-3}$, with OC at 41.12 $\mu g \cdot m^{-3}$ and EC at 13.25 $\mu g \cdot m^{-3}$ [24]. Therefore, there is an urgent need for pollution reduction measures in Delhi.

Source apportionment results for carbonaceous aerosols in Delhi show significant discrepancies, reflecting methodological challenges. Receptor models (such as Positive Matrix Factorization, PMF) applied to chemical speciation data frequently identify substantial contributions from biomass burning, vehicular emissions, and secondary formation [15, 17, 19, 23]. However, attributions to primary and secondary contributions vary widely across studies (approximately 10–40 %) [25, 26, 19, 23]. These differences may partly stem from uncertainties in emission inventories and techniques based on OC/EC ratios, which are limited by activity data and emission factors [27, 13, 28]. Hence, there is a critical need to establish objective constraint mechanisms to refine source allocation of carbonaceous aerosols, particularly to clearly distinguish contributions from fossil fuels versus contemporary biomass/biogenic sources.

Radiocarbon (^{14}C) analysis provides precisely such a constraint [29–32]. As a radioactive isotope, ^{14}C undergoes decay [33] and integrates into the modern biogeochemical cycle via atmospheric $^{14}CO_2$. In contrast, fossil-derived carbon has decayed to levels indistinguishable from instrument background over prolonged geological processes, containing negligible amounts of ^{14}C [34], enabling clear separation between fossil and non-fossil sources. This method minimizes transport-induced chemical alterations, offering robust source differentiation.

By integrating cross-seasonal $PM_{2.5}$ sampling with ^{14}C analysis in the Delhi megacity, this study aims to (1) provide isotope-based quantitative estimates of fossil and non-fossil sources with reduced methodological ambiguity, (2) further employ the extended Gelencsér (EG) method to resolve the contributions of primary versus secondary OC from these sources, particularly focusing on the role of fossil-derived POC, and (3) evaluate these ^{14}C-constrained results against conventional PMF-based apportionment [23] to identify potential biases and refine source characterization for Delhi. The findings underscore the critical need for implementing fossil-derived OC reduction strategies, particularly targeting primary emissions, and accelerating renewable energy adoption to mitigate severe carbonaceous aerosol pollution in Delhi.

2. Materials and methods

2.1. $PM_{2.5}$ sampling

Intensive $PM_{2.5}$ sampling campaigns were conducted in 2018, with samples collected at the Indian Institute of Technology Delhi (IITD: 28.54°N, 77.19°E) and Indira Gandhi Delhi Technical University for Women (IGDTUW: 28.67°N, 77.23°E) in Delhi, India. Details on the sampling sites are provided elsewhere, and both sites represent characteristic urban background locations [22, 23]. Measurements spanned three seasons: winter (January-February), pre-monsoon (March-May), and post-monsoon (October-November). Methodological details summarized in Table S1 (Supplementary Information).

To ensure comprehensive sampling, air samplers were operated simultaneously at the IITD and IGDTUW to collect $PM_{2.5}$ samples for characteristic analysis. Paired daytime (09:00–21:00, local time) and nighttime (21:00–09:00, local time) samples were collected daily, yielding 128 samples across both sites. The $PM_{2.5}$ chemical composition is characterized in detail in Srivastava, et al. (2025).

2.2. Measurement of radiocarbon (^{14}C) and calculation of EC/OC ratios

During the concurrent sampling period (26 January-1 November 2018), daytime and nighttime $PM_{2.5}$ filter samples from IITD and IGDTUW were respectively used for ^{14}C analysis and quantification of the proportion of OC versus EC on the samples. A total of 34 samples were selected for ^{14}C analysis determinations were acquired (21 from IITD and 13 from IGDTUW, Table S2) based on a stratified selection process considering season, site, and diurnal variation to ensure representativeness while accounting for measurement costs.

The proportion of OC versus EC in each sample was measured via the

hydropyrolysis (HyPy) technique. This technique has been proven to be a reliable method for isolating EC from complex environmental samples for radiocarbon analysis. Methodological comparison studies indicate that EC isolated by HyPy exhibits high consistency with results obtained via thermo-optical transmittance (TOT), a commonly used benchmark method (with an average EC/TC ratio deviation of approximately 10 %), and demonstrates superior consistency compared to other physico-chemical separation methods [35]. Data comparison in this study also reveals that the overall average difference in EC/TOC ratios measured by HyPy and conventional methods is less than 3 %, indicating that both methods capture the same carbon components within the study (Fig. S1). HyPy defines EC by selectively retaining polycyclic aromatic carbon (≥7 rings) [36, 37], thereby ensuring that the isolated component unequivocally originates from combustion processes. This approach effectively isolates EC from atmospheric aerosols, enabling its quantification and subsequent matrix-independent ^{14}C analysis of both EC and OC [38]. Samples were weighed and loaded with a catalyst (ammonium dioxydithiomolybdate [$(NH_4)_2MoO_2S_2$]). The catalyst-loaded samples were placed in pre-combusted quartz crucibles and pyrolyzed in a commercially available HyPy instrument (Strata Technology Ltd., Middlesex, UK). The HyPy reactor (containing the sample) was pressurized with hydrogen at 15 MPa. The samples were then pyrolyzed to 250°C at an initial heating rate of 300°C/min, and then heated to 550°C at 8°C/min, using a sweep gas (H_2) flow of 5 min^{-1} (ATP). The %C of the sample before and after the HyPy process was measured via elemental analysis. The proportion of EC versus OC in the sample was then calculated via the change in amount of carbon (mg C) in the starting sample versus the HyPy residue [39].

Radiocarbon measurements of OC and EC on samples were obtained by measuring the ^{14}C of the Total Carbon (TC) on the filter, and the ^{14}C of EC that had been isolated by HyPy, as described above. The ^{14}C value of OC was then obtained by difference. The ^{14}C values of TC and EC were obtained by combusting a fraction of a sample (as collected on quartz filter) before and after HyPy, respectively, in a sealed and evacuated quartz tube. This converted all organic carbon in the sample to CO_2. The sample CO_2 was cryogenically recovered and converted to graphite by Fe/Zn reduction. All sample processing was accompanied by a mixture of background and known-age standards to quantify and correct for any carbon contamination. Sample graphite was measured by Accelerator Mass Spectrometry (AMS) at either the SUERC AMS laboratory, East Kilbride, UK, or the Keck Carbon Cycle Accelerator Mass Spectrometry Facility at the University of California, Irvine, USA. Full details of the ^{14}C measurement procedure are contained in Ascough, et al. [40]. To ensure direct comparability between measurements from the two facilities, all analyses were calibrated against the same set of international standard reference materials. The reported fraction modern carbon ($F^{14}C$) values include the ±1σ total analytical uncertainty, propagated from counting statistics, standard calibration, and background corrections (Table S2).

All ^{14}C results are reported as $F^{14}C$ according to Reimer, et al. [41]. Radiocarbon values quantitatively discriminate modern biogenic carbon and fossil-derived carbon in aerosols in a two-component model. Following the Gelencsér framework [42], non-fossil fractions of EC ($f_{NF}(EC)$) and OC ($f_{NF}(OC)$) are derived from Eqs. (1) and (2), with fossil fractions of EC and OC ($f_{FF}(EC)$ and $f_{FF}(OC)$) calculated via mass balance (Eqs. (3) and (4)).

$$f_{NF}(EC) = \frac{F^{14}C}{f_{NF,\,EC}(Ref)} \quad (1)$$

$$f_{NF}(OC) = \frac{F^{14}C}{f_{NF,\,OC}(Ref)} \quad (2)$$

$$f_{FF}(EC) = 1 - f_{NF}(EC) \quad (3)$$

$$f_{FF}(OC) = 1 - f_{NF}(OC) \quad (4)$$

For EC, biomass burning is presumed the sole non-fossil source, yielding a reference $f_{NF}(EC)$ of 1.10 ± 0.05 in Eq. (1). More details on the estimation of the reference value have been reported previously [43, 33, 44–46]. For OC, the reference $f_{NF}(OC)$ in Eq. (1) is computed by Eq. (5), incorporating contributions from biomass burning ($f_{M,\,bb}$ = 1.10 ± 0.05) and biogenic source ($f_{M,\,bio}$ = 1.023 ± 0.015) [43].

$$f_{NF,\,OC}(Ref) = p_{bb} \times f_{M,\,bb} + p_{bio} \times f_{M,\,bio} \quad (5)$$

Here, p_{bb} and p_{bio} denote the proportions of biomass burning and biogenic sources, and range from 0 to 1 [47]. To quantify the sensitivity of $f_{NF,\,OC}$ to the p_{bb}, we carried out a systematic sensitivity test. By varying p_{bb} incrementally from 0 to 1 in steps of 0.01 (correspondingly, p_{bio}=1-p_{bb}) and substituting these values into Eq. (5), we calculated $f_{NF,\,OC}$. Results indicate that the calculated $f_{NF,\,OC}$ varies linearly between 1.023 (when p_{bb}=0, i.e., entirely biogenic sources) and 1.10 (when p_{bb}=1, i.e., entirely biomass burning). Considering the dominant emission characteristics of each season, we selected higher, medium, and lower p_{bb} values to calculate the specific $f_{NF,\,OC}$ for winter, pre-monsoon, and post-monsoon periods, which are 1.024, 1.044, and 1.092, respectively.

2.3. Carbonaceous aerosol source apportionment based on Extended Gelencsér (EG) method

This study employs a ^{14}C-constrained source apportionment to determine non-fossil (EC_{NF}) and fossil-derived EC (EC_{FF}), as well as OC from non-fossil (OC_{NF}) and fossil sources (OC_{FF}), using Eqs. (6)–(9).

$$EC_{NF} = f_{NF}(EC) \times EC \quad (6)$$

$$EC_{FF} = EC - EC_{NF} \quad (7)$$

$$OC_{NF} = f_{NF}(OC) \times OC \quad (8)$$

$$OC_{FF} = OC - OC_{NF} \quad (9)$$

The extended Gelencsér (EG) method further quantifies primary and secondary OC contributions from fossil sources (POC_{FF}, SOC_{FF}), as well as from OC from biomass burning (OC_{BB}) and cooking emissions (OC_{CK}) of non-fossil primary sources (Eqs. (10)–(15)). Here, the biomass burning broadly refers to the combustion process of all modern biomass fuels, including wood, straw, cow dung pellets, and similar materials. It should be clarified that the ^{14}C method cannot directly distinguish cooking emissions from other non-fossil sources, as carbon from both originates from modern biomass and exhibits identical ^{14}C characteristics. Within the EG methodology framework of this study, OC_{CK} is indirectly derived through a difference method (Eq. (15)). Consequently, OC_{CK} represents the residual fraction of POC_{NF} unexplained by biomass burning, primarily attributable to cooking activities but potentially including other unidentified minor modern primary carbon sources. This methodology has been thoroughly validated and demonstrated to be feasible in our previously published work [48].

$$POC_{FF} = EC_{FF} \times (OC/EC)_{FF,\,min} \quad (10)$$

$$SOC_{FF} = OC_{FF} - POC_{FF} \quad (11)$$

$$POC_{NF} = EC_{NF} \times (OC/EC)_{NF,\,min} \quad (12)$$

$$SOC_{NF} = OC_{NF} - POC_{NF} \quad (13)$$

$$OC_{BB} = LG \times f_{biofuels} \times (OC/LG)_{biofuels} \quad (14)$$

$$OC_{CK} = POC_{NF} - OC_{BB} \quad (15)$$

2.4. Comparing with positive matrix factorization (PMF) results

Positive Matrix Factorization (PMF) has been extensively applied in urban particulate matter source characterization studies [49–52].

Consequently, the present findings were compared with source apportionment results derived from PMF modelling to validate and discuss the performance of the EG method within complex urban environments.

For the IITD site, PMF source apportionment results based on offline $PM_{2.5}$ samples (including ions, EC/OC, metals and molecular tracers; Srivastava, et al. (2025)) will be detailed in a separate publication (Srivastava et al., in preparation). At the IGDTUW site, a High-Resolution Time-of-Flight Aerosol Mass Spectrometer (HR-ToF-AMS) was used for continuous monitoring of the composition of non-refractory submicron aerosols (PM_1), including organics, nitrate, sulfate, ammonium, and chloride. The raw AMS observation dataset is publicly accessible via the Centre for Environmental Data Analysis (CEDA) (https://catalogue.ceda.ac.uk/uuid/5631c55a2caa4cd2bcdf1bf75365bcc8). Combined with the PMF model, the uncertainties in factor profiles and contribution estimates were rigorously assessed using a bootstrap method with iterative rotation, and the results are detailed in the studies by Cash, et al. [53] and Reyes-Villegas, et al. [54].

3. Results

3.1. Overall characteristics of OC and EC

Severe fine particulate pollution was observed at both IITD and IGDTUW sites during the sampling campaigns. At IITD, the measured $PM_{2.5}$ concentrations (including both daytime and nighttime samples) ranged from 100.2 to 233.0 $\mu g \cdot m^{-3}$, 35.6–250.8 $\mu g \cdot m^{-3}$, and 89.7–294.1 $\mu g \cdot m^{-3}$ during winter, pre-monsoon and post-monsoon campaigns. IGDTUW exhibited even higher pollution levels, with $PM_{2.5}$ ranging 146.5–269.3 $\mu g \cdot m^{-3}$ (winter) and 153.5–347.7 $\mu g \cdot m^{-3}$ (post-monsoon), all 10 times more than the World Health Organization's recommended daily limit of 15 $\mu g \cdot m^{-3}$ [55].

Carbonaceous aerosols dominated $PM_{2.5}$ composition, with the combined mass of organic carbon (OC) and elemental carbon (EC) contributing 35 % (winter), 40 % (pre-monsoon), and 42 % (post-monsoon) at the IITD site. The concentrations of OC and EC averaged 38.8 ± 8.4 $\mu g \cdot m^{-3}$ and 13.6 ± 3.4 $\mu g \cdot m^{-3}$, 41.6 ± 18.7 $\mu g \cdot m^{-3}$ and 8.8 ± 3.5 $\mu g \cdot m^{-3}$, and 61.7 ± 13.0 $\mu g \cdot m^{-3}$ and 14.8 ± 4.6 $\mu g \cdot m^{-3}$ during the winter, pre-monsoon and post-monsoon campaigns, respectively (Fig. 1a). At IGDTUW, OC and EC together accounted for 32 % and 47 % of $PM_{2.5}$ mass during the sampling campaigns, with average concentrations of 49.9 ± 9.7 $\mu g \cdot m^{-3}$ and 15.9 ± 4.8 $\mu g \cdot m^{-3}$ during winter, and 86.1 ± 25.3 $\mu g \cdot m^{-3}$ and 19.7 ± 5.7 $\mu g \cdot m^{-3}$ during post-monsoon campaigns. Diurnal variation data (Fig. 1b) revealed the average OC and EC concentrations at the IITD site were 45.9 ± 13.2 $\mu g \cdot m^{-3}$ and 10.4 ± 2.9 $\mu g \cdot m^{-3}$ during the daytime, and 50.3 ± 20.8 $\mu g \cdot m^{-3}$ and 14.7 ± 5.2 $\mu g \cdot m^{-3}$ during the nighttime, respectively. At IGDTUW, OC and EC were 60.3 ± 12.1 $\mu g \cdot m^{-3}$ and 15.5 ± 4.2 $\mu g \cdot m^{-3}$ during daytime, and 76.4 ± 34.4 $\mu g \cdot m^{-3}$ and 20.3 ± 5.9 $\mu g \cdot m^{-3}$ at night. More detailed temporal variations are shown in Figs. S4–S5.

3.2. Fossil and non-fossil sources of EC and OC based on radiocarbon (^{14}C) analysis

Fig. 2 presents the temporal patterns in fossil and non-fossil fractions (f_{FF}, f_{NF}) of EC and OC. At IITD (Fig. 2a–d), fossil fuel fractions are relatively consistent across seasons, with f_{FF}(EC) and f_{FF}(OC) averaging 66 % and 63 % during the winter campaign, 62 % and 60 % during the pre-monsoon, and 63 % and 62 % during the post-monsoon campaign. Diurnal variations showed slightly higher nighttime values (66 % for EC; 64 % for OC) compared to daytime (62 %; 61 %). At IGDTUW (Fig. 2e–h), winter fossil fractions averaged at 66 % (EC) and 64 % (OC), with post-monsoon values at 66 and 66 % for EC and OC. Nighttime f_{FF}(EC) and f_{FF}(OC) were 71 % and 70 %, higher than that at IITD. Daytime values (62 % for EC; 60 % for OC) are comparable to IITD observations but remained lower than nighttime concentrations.

^{14}C-based source apportionment results for carbonaceous aerosols are presented in Fig. S6. Fossil fuel OC was the dominant contributor to total carbon, followed by OC_{NF}, EC_{FF}, and EC_{NF} across all sampling campaigns. At IITD, the contribution of OC_{FF} was 50 % during post-monsoon period, slightly higher than during winter and pre-monsoon campaigns (47 % and 48 %). Peak OC_{NF} contributions were observed during pre-monsoon (34 %), higher than that during the winter campaign (27 %). EC_{FF} was 17 %, 11 %, and 12 % during winter, pre-monsoon and post-monsoon campaigns, respectively. Biomass-related EC_{NF} remained relatively stable (7–9 %), which is highest during the winter campaign. Fossil fuel contributions at IGDTUW were enhanced during the post-monsoon campaign (OC_{FF}: 53 %, EC_{FF}: 14 %) compared to winter measurements (OC_{FF}: 51 %, EC_{FF}: 13 %). Conversely, non-fossil fuel OC and EC were slightly higher during the winter (29 %

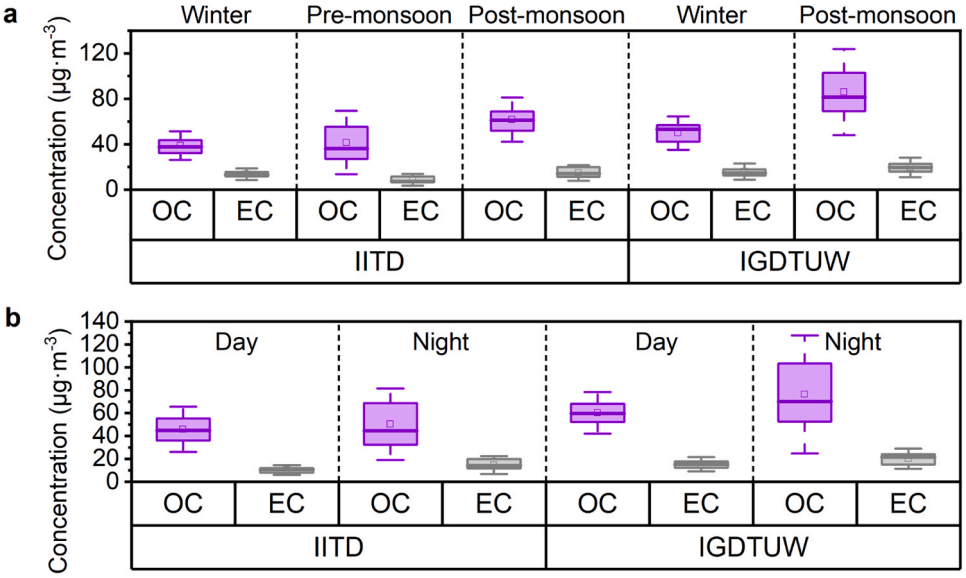

Fig. 1. Statistical characterization of OC and EC concentrations during the sampling campaigns. The boxes denote the interquartile range (25th–75th percentiles). The lower and upper limits of the whiskers indicate the standard deviation. The solid lines in the middle of the box represent the median. The hollow dots present the average values. Panel a demonstrates the seasonal trends of OC and EC at both sites, while panel b illustrates the diurnal variations of OC and EC at the two sites.

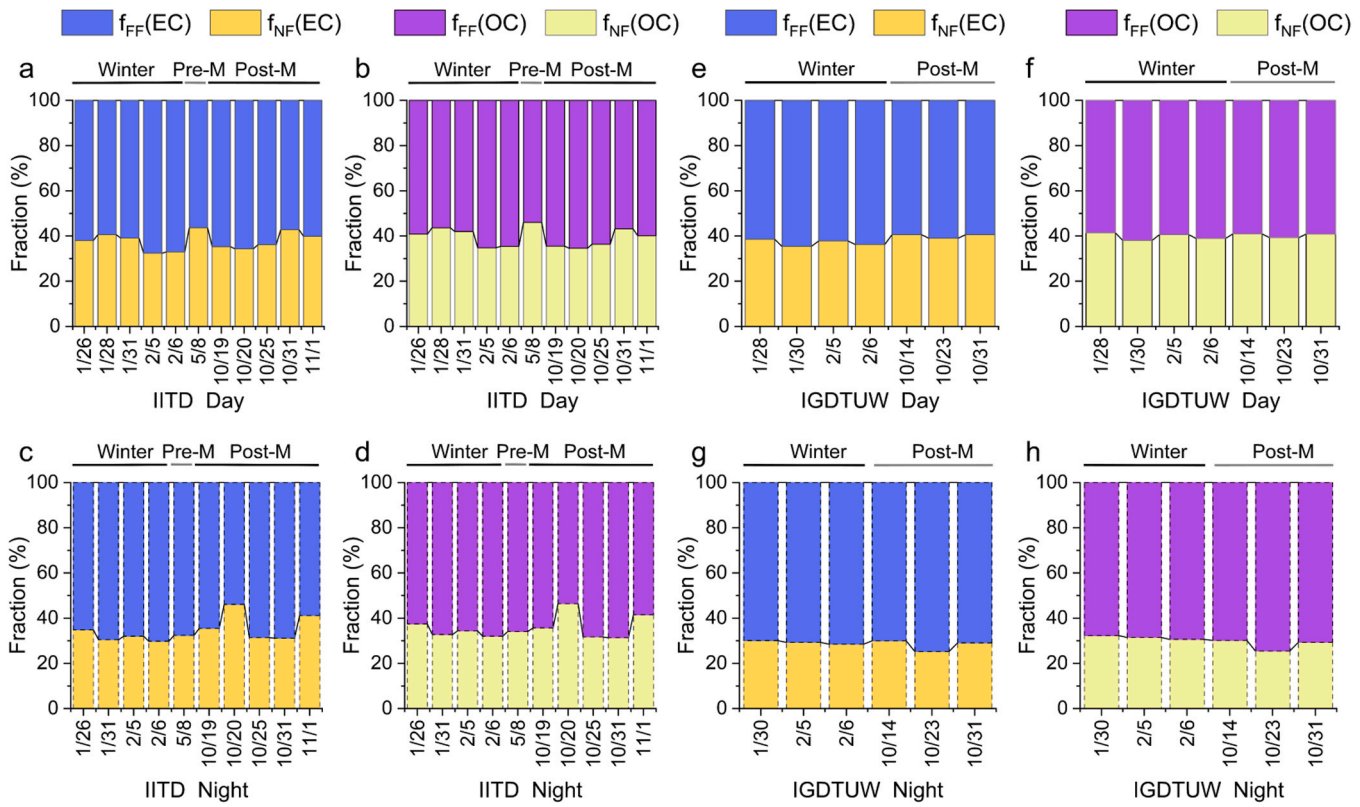

Fig. 2. Temporal variations in fossil (f_{FF}) and non-fossil (f_{NF}) fractions of EC and OC. Panels **a**–**d** display seasonal and diurnal trends at IITD site, while panels **e**–**h** show comparable data for IGDTUW. The columns in **a**, **b**, **e**, **f** represent daytime measurements, and the columns in **c**, **d**, **g**, **h** are displayed during nighttime.

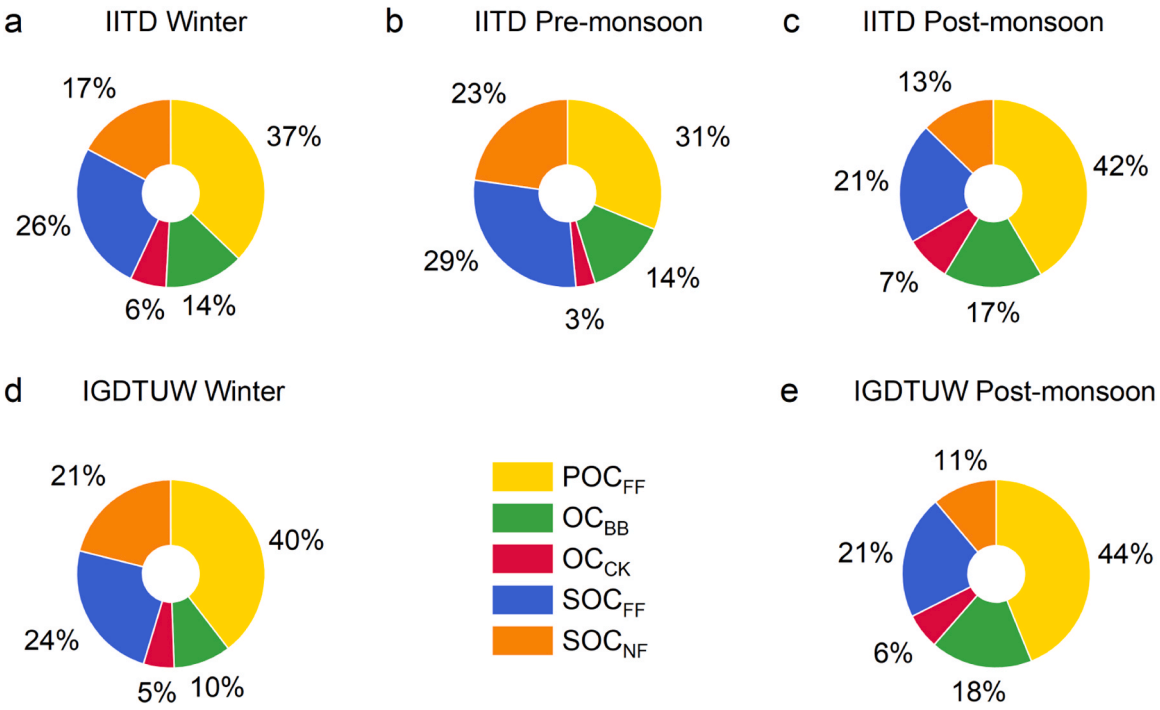

Fig. 3. Source-resolved OC contributions (%) from POC_{FF}, SOC_{FF}, SOC_{NF}, OC_{BB}, and OC_{CK}. Panels a–c represent the source contributions during winter, pre-monsoon, and post-monsoon campaigns at the IITD site. Panels d–e represent the source contributions during winter and post-monsoon campaigns at the IGDTUW site. The contributions from fossil and non-fossil fuel sources are further categorized as POC_{FF} (primary organic carbon from fossil fuels), SOC_{FF} (secondary organic carbon from fossil fuels), SOC_{NF} (secondary organic carbon from non-fossil fuels), OC_{BB} (biomass burning organic carbon), and OC_{CK} (cooking-derived organic carbon). Notably, OC_{BB} and OC_{CK} together constitute POC_{NF} (primary organic carbon from non-fossil fuels) [48].

and 7 %) than during the post-monsoon campaign (27 % and 6 %).

3.3. Fossil and non-fossil sources of POC and SOC

Fig. 3 illustrates the relative contributions of POC and SOC using the Extended Gelencsér method (EG) method, revealing distinct seasonal and site-specific source patterns. Overall, fossil-derived primary OC (POC_{FF}) consistently remained the dominant contributor to OC, ranging from 31 to 42 % at IITD site (Fig. 3a–c) and 40–44 % at IGDTUW site (Fig. 3d–e). Fossil-related secondary OC (SOC_{FF}) accounted for 21–29 % at IITD and 21–24 % at IGDTUW, which aligns with observations from Chinese megacities [56–58]. Non-fossil secondary OC (SOC_{NF}) also constituted a notable proportion, contributing 13–23 % at IITD and 11–21 % at IGDTUW. Furthermore, OC_{BB} contributed 10–18 % distinguished via the EG method, while OC_{CK} remained a minor source, accounting for only 3–7 % (see Text S2 for details).

Seasonal analysis at the IITD site showed that the mean contribution of POC_{FF} was highest during the post-monsoon period (concentration: 29.90 $\mu g \cdot m^{-3}$, accounting for 42 % of total sources), higher than that during the winter (37 %, 16.99 $\mu g \cdot m^{-3}$) and pre-monsoon campaigns (31 %, 11.45 $\mu g \cdot m^{-3}$) (Fig. 3a–c). The corresponding contributions for SOC_{FF} peaked in pre-monsoon (29 %), with winter and post-monsoon contributions at 26 % and 21 %, respectively. SOC_{NF} exhibited a similar trend, contributing most during the pre-monsoon period (23 %), followed by winter (17 %), and least in the post-monsoon period (13 %). OC_{BB} contributions remained relatively stable, with 14 % in both winter (6.45 $\mu g \cdot m^{-3}$) and pre-monsoon (5.38 $\mu g \cdot m^{-3}$), rising slightly to 17 % post-monsoon (13.53 $\mu g \cdot m^{-3}$). OC_{CK} maintained low levels across all seasons (3–7 %, with concentrations of 2.75 $\mu g \cdot m^{-3}$ in winter, 1.76 $\mu g \cdot m^{-3}$ pre-monsoon, and 6.26 $\mu g \cdot m^{-3}$ post-monsoon). At the IGDTUW site (Fig. 3d–e), POC_{FF} contributed most during the post-monsoon period (44 %, 40.61 $\mu g \cdot m^{-3}$), compared to 40 % in winter. SOC_{FF} was slightly higher in winter than (24 %) than post-monsoon campaign (21 %). SOC_{NF} showed pronounced seasonal differences, contributing 21 % in winter but only 11 % during the pre-monsoon campaign. Among primary non-fossil sources, the average contribution of OC_{BB} was higher during the post-monsoon (18 %, 14.55 $\mu g \cdot m^{-3}$) than in winter (10 %, 5.02 $\mu g \cdot m^{-3}$). OC_{CK} showed minimal seasonal variation, remaining at 5 % and 6 % (2.64 $\mu g \cdot m^{-3}$ in winter and 4.92 $\mu g \cdot m^{-3}$ in the post-monsoon period).

4. Discussion

4.1. Validation and discussion of ^{14}C-based source apportionment results

This study employed the ^{14}C-based EG method and PMF model to analyze the sources of OC in $PM_{2.5}$ at two sites (offline data for IITD site, and AMS data for IGDTUW site). Although the two methods differ inherently in principle and measurement, they proved to be effectively complementary and mutually verifiable. By evaluating their key findings and discrepancies, the capability of the ^{14}C method in distinguishing between fossil and non-fossil carbon contributions can be

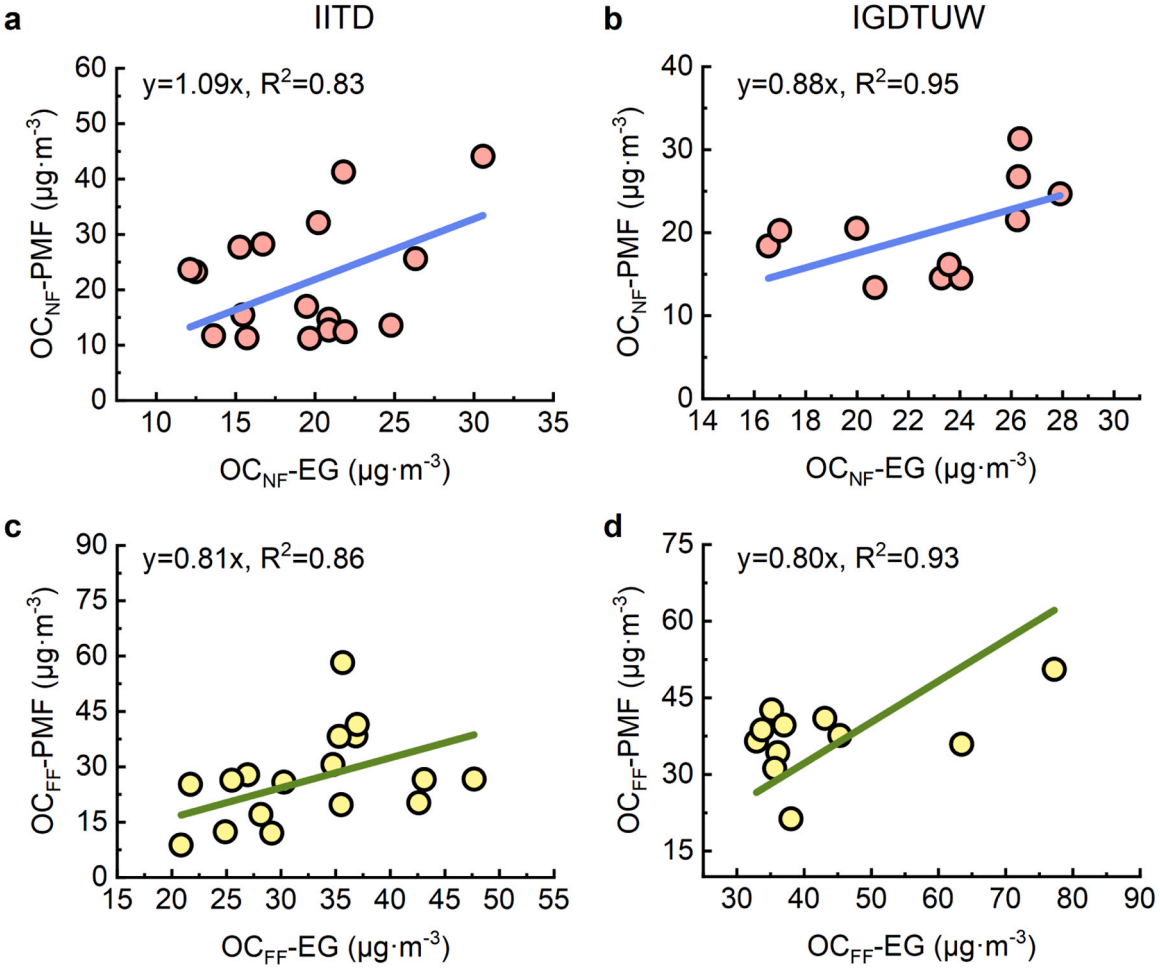

Fig. 4. Correlations of OC_{NF} and OC_{FF} source contributions (unit: $\mu g \cdot m^{-3}$) obtained using the extended Gelencsér method (EG) and PMF method (offline chemical composition at IITD and AMS at IGTUW) during sampling. Here, EG-resolved contributions are labelled as OC_{NF}-EG and OC_{FF}-EG, while PMF-derived values are denoted OC_{NF}-PMF and OC_{FF}-PMF, respectively.

further revealed, thereby deepening the understanding of pollution formation in Delhi. The PMF model resolved sources including crop burning, cooking, industrial chloride emissions, solid waste burning, dust, secondary inorganics, solid fuel combustion, industrial activities, plastic related aerosols, and transport (Materials and methods). Among these, the PMF-resolved sources of industrial activities, plastic related aerosols, solid fuel combustion, and transport were categorized as POC_{FF}, cooking as OC_{CK}, and crop burning as OC_{BB}. The seasonal (winter, pre-monsoon, post-monsoon) contributions of OC sources resolved by PMF at the two sites are detailed in Table S5.

Overall, the two methods showed well correlation (correlation coefficient >0.8) in quantifying contributions of non-fossil organic carbon (OC_{NF}) and fuel-derived organic carbon (OC_{FF}) to $PM_{2.5}$, but significant differences were observed at the individual sample level (Fig. 4). At the IITD site, the OC_{NF} contribution resolved by PMF was on average 1.2 times that of the EG method (range 0.5–3.0 times), while the OC_{FF} contribution was on average 0.8 times (range 0.6–2.4 times). At the IGDTUW site, the results from the two methods were more consistent, with the average OC_{NF} and OC_{FF} contributions resolved by PMF both being 0.9 times those of the EG method, with ranges between 0.8–1.7 times and 0.8–1.8 times, respectively.

Further comparison of specific sources revealed that the primary fossil OC (POC_{FF}) contribution quantified by the PMF method was generally systematically higher than that by the EG method (Fig. 5). At the IITD site, the POC_{FF}-PMF contribution was 1.2–3.6 times that of POC_{FF}-EG; at the IGDTUW site, this ratio ranged from 0.9 to 1.3. For OC_{CK}, the seasonal trends quantified by the two methods were similar, with relatively stable contributions. The contribution values ranged from 3 to 7 % at the IITD site and 5–6 % at the IGDTUW site (Fig. 5), reflecting the persistence and spatial uniformity of residential emissions [59]. Although the OC_{CK} contribution derived by the PMF method was slightly lower, this may relate to its difficulty in fully separating traffic and cooking emissions [60–62]. For OC_{BB}, the two methods yielded relatively consistent estimates during winter and the pre-monsoon season. However, during the post-monsoon season, the PMF results were significantly higher than those from the EG method, exceeding them by 2.1 times and 1.7 times at the IITD and IGDTUW sites, respectively (Fig. 5).

The quantitative differences described above stem from the distinct methodological characteristics and inherent uncertainties of the two approaches [63, 64]. The uncertainty of the EG method primarily relies on the selection of key parameters [65–67]. The quantification of POC_{FF} is sensitive to the chosen $(OC/EC)_{FF,\ min}$ ratio, which may vary with different fossil fuel combustion processes and seasons. The derivation of OC_{BB} is highly dependent on specific OC/levoglucosan ratio, which shows significant differences depending on fuel type (e.g., wood vs. straw) and combustion conditions [48]. This study assumed a simplified scenario dominated by wood/straw mixtures (Fig. S3, Table S4), yet this can still introduce uncertainty into the OC_{BB} calculation. Furthermore, the limited sample during the pre-monsoon period may have affected the comparative results for this season.

The uncertainties associated with the AMS-PMF technique manifest in several aspects. The PMF resolution process involves subjectivity, particularly in factor identification and interpretation [8], which may account for the considerable variability in results at the IITD site and the potential overestimation of POC_{FF}. For the IGDTUW site utilizing AMS data, uncertainties in the relative ionization efficiency (RIE) and collection efficiency (CE) affect quantitative accuracy [68]. More importantly, AMS struggles to distinguish sources with similar mass spectral characteristics. For instance, the similarity in mass spectral signatures between cooking and vehicular emissions [60–62] may lead to some OC_{CK} being misattributed to the POC_{FF} factor. Furthermore, the similarity in mass spectra between biomass burning organic aerosol (BBOA) and various types of oxidized organic aerosol (OOA) may lead to factor misallocation during PMF analysis [63, 69, 70], which could partly explain the significant discrepancy in OC_{BB} during the post-monsoon season. Systematic differences between the two methods also include variations in particle size cutoffs (AMS targets PM_1, whereas ^{14}C analysis targets $PM_{2.5}$).

4.2. *The dominant contribution of fossil fuel and its spatial-temporal variations*

Fossil fuel combustion has been identified as the dominant source of OC and EC in Delhi (Fig. 2). Spatial monitoring data indicates that at IITD site, fossil fuel contributions averaged ~65 % for EC and ~60 % for OC, whereas IGDTUW recorded slightly higher values, around 70 % for both species. This spatial variation is primarily attributed to differences in local emission source characteristics and microenvironmental factors. The IGDTUW site is situated in a high-density urban area and hosts various fossil fuel combustion sources, such as vehicular traffic and commercial activities, which are the dominant contributors to EC and OC production at this location [71]. Conversely, IITD might be influenced by mixed sources, including regional transport and lower traffic density [72], resulting in slightly lower fossil source signatures. These findings align with broader observations that urban infrastructure and emission hotspots drive spatial variability of EC and OC in megacities [73, 48]. Notably, IGDTUW's proximity to major traffic networks, with heavy vehicular traffic further amplifying fossil fuel combustion emissions, is significant as diesel generators and heavy-duty vehicles are known emitters of high EC [74]. These results emphasize the importance of implementing localized emission controls strategies tailored to site-specific source characteristics.

On a temporal scale, both sites observed clear diurnal variations in fossil fuel contributions to EC and OC, with consistently higher nighttime contributions (Fig. 2). Specifically, at the IITD site, the nighttime f_{FF}(EC) was 66 % (EC_{FF}=11.4 μg·m^{-3}), which decreased to 62 % during the daytime (EC_{FF}=7.3 μg·m^{-3}). At the IGDTUW site, the nocturnal

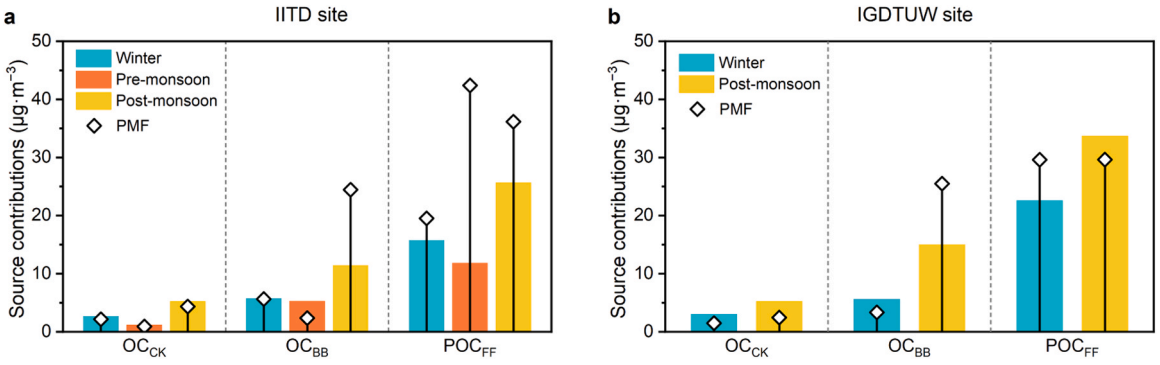

Fig. 5. Comparison of the OC_{CK}, OC_{BB}, and POC_{FF} source contributions (unit: μg·m^{-3}) derived by EG method (coloured bars) and PMF method (diamonds) based on identical sampling periods.

f_{FF}(EC) reached as high as 71 % (EC_{FF}=13.1 μg·m^{-3}), while it similarly dropped to 62 % during the day (EC_{FF}=9.0 μg·m^{-3}). The concentrations of OC_{FF} also exhibited the same trend, with significantly higher nocturnal concentrations (IITD: 34.2 μg·m^{-3}; IGDTUW: μg·m^{-3}) compared to daytime levels (IITD: 30.5 μg·m^{-3}; IGDTUW: μg·m^{-3}). The persistent daytime contributions may be primarily attributable to traffic activity and potential industrial emissions [75]. The marked increase in the proportion of fossil fuel contributions at night likely indicates a shift in source emission mechanisms or intensities [56]. A plausible hypothesis for the marked increase in fossil fuel contributions at night is the local traffic regulation that restricts heavy-duty vehicles (HDVs, predominantly diesel-powered) from entering the city center during daytime, potentially concentrating their activity during nighttime hours [76, 77, 57]. Furthermore, the elevated contribution of EC_{FF} in winter (e.g., 17 % at IITD site) is likely associated with increased diesel generator usage [78–80] and incomplete fuel combustion under lower temperatures [81]. In addition to changes in emission sources, meteorological conditions like nocturnal boundary layer compression may significantly elevate ambient concentrations by limiting pollutant dispersion [82–84].

In contrast to some isotopic studies in South Asia [85, 86], our research observed a higher contribution from OC_{FF} than from EC_{FF}. The discrepancy primarily stems from differences in the study region and atmospheric processes. Our study focuses on the urban area of Delhi, characterized by intensive fossil fuel consumption and complex emission sources, including heavy-duty diesel vehicles, coal combustion, and industrial activities [22, 23]. These sources emit not only EC directly but also substantial amounts of fossil-derived primary OC (POC_{FF}), accounting for 31–44 % of total OC (Fig. 3). More importantly, under Delhi's highly polluted conditions, secondary organic carbon (SOC_{FF}) formed from the photochemical oxidation of fossil precursors contributes significantly, representing 21–29 % of OC, thereby substantially increasing the total OC_{FF}. In comparison, studies at regional background sites typically sample aged air masses after long-range transport, during which volatile components may be lost or transformed, resulting in a fossil fuel signal more concentrated in stable EC.

In summary, the findings of this study highlight that intense local emissions coupled with active secondary formation processes are key drivers behind the high-OC characteristic of fossil fuel contributions in the heavily polluted core of a megacity.

4.3. Lower than expected role of biomass burning

Although multiple studies focusing on northern Indian regions (e.g., Punjab, Kanpur, Rohtak, Mohali) have highlighted biomass burning as a dominant source of total carbonaceous aerosols [87–91], this study observed that OC_{BB} accounted for 10–18 % of OC in Delhi (Fig. 3). This conclusion aligns with findings from Srivastava, et al. (2025). During peak burning seasons (winter and late monsoon), OC_{BB} contributions showed only slight increases without significant growth (e.g., 14 % in winter and 17 % in the post-monsoon period at the IITD site). This is primarily attributed to the strong and seasonally intensified fossil fuel emissions in Delhi. Under unfavorable meteorological conditions, such as lower mixing layer height and reduced wind speed [23], the concentrations of fossil-derived OC (particularly POC_{FF}) from local traffic, heating, and industrial emissions increase substantially, diluting the relative growth in OC_{BB} contribution. Furthermore, the weak correlation between OC_{BB} and $PM_{2.5}$ shown in Fig. S7 indicates that OC_{BB} is not the dominant driver of severe haze events.

Nevertheless, this result contrasts with multiple receptor modelling studies (Table S6) that identify biomass burning as a primary source of Delhi's $PM_{2.5}$ [92, 26, 93, 94]. The discrepancy likely stems primarily from methodological differences in source apportionment. Receptor modelling is susceptible to subjective influences and may misattribute other sources to OC_{BB} [8]. Moreover, OC_{BB} calculations based on LG (Eq. (14)) are sensitive to biomass fuel type, inevitably introducing uncertainty. For instance, studies demonstrate that wood combustion yields higher OC/LG ratios than crop straw, potentially leading to underestimation of OC_{BB} when mixed fuels dominate [48]. However, in this study, the contribution of non-fossil carbon is directly constrained by ^{14}C data, thereby confining OC_{BB} within a reasonable range and avoiding potential biases associated with relying solely on the OC/LG ratio. Under these constraints (Table S4), both OC_{BB} and OC_{CK} obtained via the difference method yield reasonable physical interpretations, enhancing the robustness of the results.

In summary, although the contribution of biomass burning was lower than anticipated, the elevated OC_{BB} levels still coincided temporally with the peak straw-burning period. This indicates that regional biomass burning events continue to exert a discernible impact on urban areas.

4.4. Seasonal dynamics of secondary aerosols and potential driving factors

The source apportionment results obtained using the EG method reveal distinct seasonal patterns in SOC. Specifically, SOC_{NF} exhibits its highest contribution during the pre-monsoon period (accounting for 23 % of OC), while SOC_{FF} shows a significantly higher contribution in winter (24–26 %) compared to the post-monsoon period (11–13 %). At the IGDTUW site, the contribution of SOC_{FF} remains relatively stable across seasons (21–24 %). It should be noted that this study did not involve specialized model simulations or flux measurements of SOC formation processes (such as oxidation rates or gas-particle partitioning coefficients). Therefore, the following mechanistic explanations for the observed seasonal patterns are reasonable inferences based on the observational data and established atmospheric chemistry knowledge.

The peak in SOC_{NF} during the pre-monsoon season potentially linked to higher temperatures, stronger solar radiation, and enhanced emissions of biogenic VOCs during this period [95]. The elevated contribution of SOC_{FF} in winter can be explained through atmospheric physicochemical processes. Low-temperature environments typically enhance the gas-particle partitioning efficiency of semi-volatile organic compounds, thereby promoting their conversion to particulate matter [96]. In contrast, the contribution of SOC_{FF} remained relatively stable across seasons, potentially reflecting distinct precursor sources compared to SOC_{NF}. Fossil-derived VOCs primarily originate from relatively stable emission sources such as transport, exhibiting minimal seasonal fluctuations in emission fluxes. Consequently, their secondary formation processes are governed more by factors with smaller relative variations, such as oxidant concentrations [97, 98], rather than being significantly influenced by direct meteorological conditions like their biogenic precursors.

Future research integrating high-resolution meteorological observations, precursor measurements, and photochemical models would help quantitatively verify these processes and clarify the relative importance of each contributing factor.

5. Conclusion and implication

This study employs radiocarbon isotope analysis to provide key constraints on the sources of carbonaceous aerosols in Delhi, quantitatively revealing the spatiotemporal distribution characteristics of fossil and non-fossil contributions. The results indicate that fossil fuel combustion substantially contributes to carbonaceous aerosols in Delhi, accounting for 62–65 % of OC and 64–66 % of EC. Among these, POC_{FF} is the most important single component, constituting 31–44 % of OC and exhibiting a pronounced concentration peak during the late monsoon period. The finding confirms the dominant role of fossil fuels in Delhi's air pollution and their seasonal dynamics, providing critical scientific evidence for formulating targeted sectoral emission reduction strategies in this megacity.

The study further compares the results of the EG and PMF methods. Although both methods are consistent in identifying the overall trends of

major OC sources (fossil and non-fossil), differences exist in the quantitative contributions of specific sources (e.g., POC_{FF} and OC_{BB}). These differences reflect the respective strengths and limitations of the two approaches. The EG method based on radiocarbon offers a more direct and objective in distinguishing fossil from non-fossil carbon, but its results depend on the selection of key parameters. The PMF method can resolve more detailed source categories, but its results are susceptible to the influence of model assumptions and the subjectivity of factor identification. Therefore, in complex emission environments like Delhi, the combined application of both methods alongside a careful assessment of their uncertainties is crucial for precise source tracing.

Our study indicates that while biomass burning control remains essential (e.g., OC_{BB} alone exceeds WHO $PM_{2.5}$ annual average guidelines), fossil fuel combustion should be prioritized as the primary target for emissions reduction in Delhi. Particularly given that the data collection occurred in 2018, prior to the nationwide shift from BS-IV to BS-VI fuel and vehicle emission standards in 2020, these findings provide a valuable pre-policy baseline for evaluating the effectiveness of such policy interventions aimed at reducing motor vehicle emissions. Future studies applying carbon isotope or radiocarbon-based methods post-2020, will be crucial to examine whether the contribution of fossil fuel-related $PM_{2.5}$ has declined post-intervention.

In summary, the innovation of this study lies in achieving a refined quantitative estimation of pollution source contributions through isotopic constraints. It not only clarifies the central role of primary emissions from fossil sources but also suggests that traditional methods may tend to overestimate the contribution of biomass burning. These insights reinforce the priority of pollution control pathways centered on energy transition and key industry upgrades, providing solid scientific support for effectively reducing carbonaceous aerosol loads and improving air quality.

Environmental Implication

This study underscores fossil fuel combustion (e.g., from traffic or power plants) as the dominant contributor to organic carbon in Delhi's $PM_{2.5}$ through radiocarbon-based source apportionment, revealing higher contributions than previous estimates, particularly post-monsoon. The findings highlight that prioritizing fossil fuel control via clean energy transitions and electric mobility offers greater air quality co-benefits than biomass burning or cooking emission interventions. These seasonal insights provide targeted policy support for heavily polluted megacities and establish benchmarks for evaluating future emissions regulations. Post-2020 isotopic tracking remains essential to evaluate fossil-derived PM reductions and refine control strategies.

Declaration of Competing Interest

The authors declare that they have no known competing financial interests or personal relationships that could have appeared to influence the work reported in this paper.

Acknowledgments

This work has been supported by the Natural Environmental Research Council as a part of the UK-India NERC-MoES Programme via the project 'An Integrated Study of Air Pollutant Sources in the Delhi National Capital Region (ASAP-Delhi)' funded under the grant numbers NE/P016499/1 and NE/P016510/1. We acknowledge support from NERC via the National Environmental Isotope Facility (NEIF) grant funding (NE/S011587/1), NEIF project allocation number 2146.1018. Authors gratefully acknowledge the financial support provided by the Earth System Science Organization, MoES, Government of India, under the India-UK joint collaboration for conducting this research. We acknowledge the support of Dr. Sarkawt Hama during sampling activites in Delhi. We would also like to thank the technical superintendent of the Environmental Engineering Lab at the Civil Engineering Department of IIT Delhi for their support during ambient monitoring. Additionally, we acknowledge the support of the staff at the Department of Applied Sciences and Humanities, IGDTUW, for providing access to the sampling site. We also gratefully acknowledge support from the Nankai University Blue Sky Foundation (China).

Appendix A. Supporting information

Supplementary data associated with this article can be found in the online version at doi:10.1016/j.jhazmat.2026.141289.

Data availability

Data will be made available on request.

References

[1] Balakrishnan, K., Dey, S., Gupta, T., Dhaliwal, R.S., Brauer, M., Cohen, A.J., Stanaway, J.D., Beig, G., Joshi, T.K., Aggarwal, A.N., Sabde, Y., Sadhu, H., Frostad, J., Causey, K., Godwin, W., Shukla, D.K., Kumar, G.A., Varghese, C.M., Muraleedharan, P., Agrawal, A., Anjana, R.M., Bhansali, A., Bhardwaj, D., Burkart, K., Cercy, K., Chakma, J.K., Chowdhury, S., Christopher, D.J., Dutta, E., Furtado, M., Ghosh, S., Ghoshal, A.G., Glenn, S.D., Guleria, R., Gupta, R., Jeemon, P., Kant, R., Kant, S., Kaur, T., Koul, P.A., Krish, V., Krishna, B., Larson, S. L., Madhipatla, K., Mahesh, P.A., Mohan, V., Mukhopadhyay, S., Mutreja, P., Naik, N., Nair, S., Nguyen, G., Odell, C.M., Pandian, J.D., Prabhakaran, D., Prabhakaran, P., Roy, A., Salvi, S., Sambandam, S., Saraf, D., Sharma, M., Shrivastava, A., Singh, V., Tandon, N., Thomas, N.J., Torre, A., Xavier, D., Yadav, G., Singh, S., Shekhar, C., Vos, T., Dandona, R., Reddy, K.S., Lim, S.S., Murray, C.J.L., Venkatesh, S., Dandona, L., 2019. The impact of air pollution on deaths, disease burden, and life expectancy across the states of India: The global burden of disease study 2017. Lancet Planet Heath 3 (1), e26–e39.

[2] Guo, S., Hu, M., Levy Zamora, M., Peng, J., Shang, D., Zheng, J., Du, Z., Wu, Z., Shao, M., Zeng, L., Molina, M., Zhang, R., 2014. Elucidating severe urban haze formation in China. Proc Natl Acad Sci 111 (49), 17373–17378.

[3] Wang, Y., Zhang, R., Saravanan, R., 2014. Asian pollution climatically modulates mid-latitude cyclones following hierarchical modelling and observational analysis. Nat Commun 5 (1), 3098.

[4] Hu, W., Zhao, Y., Lu, N., Wang, X., Zheng, B., Henze, D.K., Zhang, L., Fu, T.-M., Zhai, S., 2024. Changing responses of $PM_{2.5}$ and ozone to source emissions in the Yangtze River Delta using the adjoint model. Environ Sci Technol 58 (1), 628–638.

[5] Manisalidis, I., Stavropoulou, E., Stavropoulos, A., Bezirtzoglou, E., 2020. Environmental and health impacts of air pollution: A review. Front Public Health 8, 14.

[6] Pope Iii, C.A., Dockery, D.W., 2006. Health effects of fine particulate air pollution: Lines. that Connect J Air Waste Manag Assoc 56 (6), 709–742.

[7] Zhang, Y., Vu, T.V., Sun, J., He, J., Shen, X., Lin, W., Zhang, X., Zhong, J., Gao, W., Wang, Y., Fu, T.M., Ma, Y., Li, W., Shi, Z., 2020. Significant changes in chemistry of fine particles in wintertime Beijing from 2007 to 2017: Impact of clean air actions. Environ Sci Technol 54 (3), 1344–1352.

[8] Zhang, Y., Zhang, X., Zhong, J., Sun, J., Shen, X., Zhang, Z., Xu, W., Wang, Y., Liang, L., Liu, Y., Hu, X., He, M., Pang, Y., Zhao, H., Ren, S., Shi, Z., 2022. On the fossil and non-fossil fuel sources of carbonaceous aerosol with radiocarbon and AMS-PMF methods during winter hazy days in a rural area of North China plain. Environ Res 208, 112672.

[9] Szidat, S., 2009. Sources of Asian haze. Science 323 (5913), 470–471.

[10] Cao, J.J., Lee, S.C., Chow, J.C., Watson, J.G., Ho, K.F., Zhang, R.J., Jin, Z.D., Shen, Z.X., Chen, G.C., Kang, Y.M., Zou, S.C., Zhang, L.Z., Qi, S.H., Dai, M.H., Cheng, Y., Hu, K., 2007. Spat Seas Distrib Carbon Aerosols China J Geophys Res Atmos 112, D22S11.

[11] Zhang, X.Y., Wang, Y.Q., Zhang, X.C., Guo, W., Gong, S.L., 2008. Carbonaceous aerosol composition over various regions of China. 2006 J Geophys Res Atmos 113, D14111.

[12] Turpin, B.J., Huntzicker, J.J., 1995. Identification of secondary organic aerosol episodes and quantitation of primary and secondary organic aerosol concentrations during SCAQS. Atmos Environ 29 (23), 3527–3544.

[13] Bond, T.C., Streets, D.G., Yarber, K.F., Nelson, S.M., Woo, J.-H., Klimont, Z., 2004. A technology-based global inventory of black and organic carbon emissions from combustion. J Geophys Res Atmos 109, D14203.

[14] Balachandran, S., Pachon, J.E., Lee, S., Oakes, M.M., Rastogi, N., Shi, W., Tagaris, E., Yan, B., Davis, A., Zhang, X., Weber, R.J., Mulholland, J.A., Bergin, M. H., Zheng, M., Russell, A.G., 2013. Particulate and gas sampling of prescribed fires in South Georgia, USA. Atmos Environ 81, 125–135.

[15] Gadi, R., Shivani, Sharma, S.K., Mandal, T.K., 2019. Source apportionment and health risk assessment of organic constituents in fine ambient aerosols ($PM_{2.5}$): A complete year study over National Capital Region of India. Chemosphere 221, 583–596.

[16] Goel, V., Jain, S., Singh, V., Kumar, M., 2023. Source apportionment, health risk assessment, and trajectory analysis of black carbon and light absorption properties

of black and brown carbon in Delhi, India. Environ Sci Pollut Res 30 (54), 116252–116265.
[17] Gupta, S., Gadi, R., Sharma, S.K., Mandal, T.K., 2018. Characterization and source apportionment of organic compounds in PM_{10} using PCA and PMF at a traffic hotspot of Delhi. Sustain Cities Soc 39, 52–67.
[18] Jain, S., Sharma, S.K., Mandal, T.K., Saxena, M., 2018. Source apportionment of PM_{10} in Delhi, India using PCA/APCS, UNMIX and PMF. Particuology 37, 107–118.
[19] Lalchandani, V., Srivastava, D., Dave, J., Mishra, S., Tripathi, N., Shukla, A.K., Sahu, R., Thamban, N.M., Gaddamidi, S., Dixit, K., Ganguly, D., Tiwari, S., Srivastava, A.K., Sahu, L., Rastogi, N., Gargava, P., Tripathi, S.N., 2022. Effect of biomass burning on $PM_{2.5}$ composition and secondary aerosol formation during post-monsoon and winter haze episodes in Delhi. J Geophys Res Atmos 127 (1) e2021JD035232.
[20] Pandey, A., Brauer, M., Cropper, M.L., Balakrishnan, K., Mathur, P., Dey, S., Turkgulu, B., Kumar, G.A., Khare, M., Beig, G., Gupta, T., Krishnankutty, R.P., Causey, K., Cohen, A.J., Bhargava, S., Aggarwal, A.N., Agrawal, A., Awasthi, S., Bennitt, F., Bhagwat, S., Bhanumati, P., Burkart, K., Chakma, J.K., Chiles, T.C., Chowdhury, S., Christopher, D.J., Dey, S., Fisher, S., Fraumeni, B., Fuller, R., Ghoshal, A.G., Golechha, M.J., Gupta, P.C., Gupta, R., Gupta, R., Gupta, S., Guttikunda, S., Hanrahan, D., Harikrishnan, S., Jeemon, P., Joshi, T.K., Kant, R., Kant, S., Kaur, T., Koul, P.A., Kumar, P., Kumar, R., Larson, S.L., Lodha, R., Madhipatla, K.K., Mahesh, P.A., Malhotra, R., Managi, S., Martin, K., Mathai, M., Mathew, J.L., Mehrotra, R., Mohan, B.V.M., Mohan, V., Mukhopadhyay, S., Mutreja, P., Naik, N., Nair, S., Pandian, J.D., Pant, P., Perianayagam, A., Prabhakaran, D., Prabhakaran, P., Rath, G.K., Ravi, S., Roy, A., Sabde, Y.D., Salvi, S., Sambandam, S., Sharma, B., Sharma, M., Sharma, S., Sharma, R.S., Shrivastava, A., Singh, S., Singh, V., Smith, R., Stanaway, J.D., Taghian, G., Tandon, N., Thakur, J.S., Thomas, N.J., Toteja, G.S., Varghese, C.M., Venkataraman, C., Venugopal, K.N., Walker, K.D., Watson, A.Y., Wozniak, S., Xavier, D., Yadama, G.N., Yadav, G., Shukla, D.K., Bekedam, H.J., Reddy, K.S., Guleria, R., Vos, T., Lim, S.S., Dandona, R., Kumar, S., Kumar, P., Landrigan, P.J., Dandona, L., 2021. Health and economic impact of air pollution in the states of India: The global burden of disease study 2019. Lancet Planet Heath 5 (1), e25–e38.
[21] Sharma, S.K., Gupta, S., Tiwari, P., Banoo, R., Rai, A., Vijayan, N., 2025. Characteristics, sources and reconstruction of primary & secondary components of $PM_{2.5}$ in Delhi, India. J Atmos Chem 82 (2), 14.
[22] Shukla, A.K., Tripathi, S.N., Canonaco, F., Lalchandani, V., Sahu, R., Srivastava, D., Dave, J., Thamban, N.M., Gaddamidi, S., Sahu, L., Kumar, M., Singh, V., Rastogi, N., 2023. Spatio-temporal variation of C-$PM_{2.5}$ (composition based $PM_{2.5}$) sources using PMF*PMF (double-PMF) and single-combined PMF technique on real-time non-refractory, BC and elemental measurements during post-monsoon and winter at two sites in Delhi, India. Atmos Environ 293, 119456.
[23] Srivastava, D., Alam, M.S., Rooney, D.J., Crilley, L.R., Kramer, L., Saksakulkrai, S., Dhawan, S., Khare, Shivani, M., Gadi, R., Kumar, P., Hama, S., Harrison, R.M., Shi, Z., Bloss, W.J., 2025. The influence of local and regional sources on concentrations of fine particulate matter in Delhi. Atmos Pollut Res 16 (7), 102476.
[24] Mandal, P., Sarkar, R., Mandal, A., Saud, T., 2014. Seasonal variation and sources of aerosol pollution in Delhi, India. Environ Chem Lett 12 (4), 529–534.
[25] Bikkina, S., Andersson, A., Kirillova, E.N., Holmstrand, H., Tiwari, S., Srivastava, A. K., Bisht, D.S., Gustafsson, Ö., 2019. Air quality in megacity Delhi affected by countryside biomass burning. Nat Sustain 2 (3), 200–205.
[26] Jain, S., Sharma, S.K., Vijayan, N., Mandal, T.K., 2021. Investigating the seasonal variability in source contribution to $PM_{2.5}$ and PM_{10} using different receptor models during 2013–2016 in Delhi, India. Environ Sci Pollut Res 28 (4), 4660–4675.
[27] Bond, T.C., Doherty, S.J., Fahey, D.W., Forster, P.M., Berntsen, T., DeAngelo, B.J., Flanner, M.G., Ghan, S., Kärcher, B., Koch, D., Kinne, S., Kondo, Y., Quinn, P.K., Sarofim, M.C., Schultz, M.G., Schulz, M., Venkataraman, C., Zhang, H., Zhang, S., Bellouin, N., Guttikunda, S.K., Hopke, P.K., Jacobson, M.Z., Kaiser, J.W., Klimont, Z., Lohmann, U., Schwarz, J.P., Shindell, D., Storelvmo, T., Warren, S.G., Zender, C.S., 2013. Bounding the role of black carbon in the climate system: A scientific assessment. J Geophys Res Atmos 118 (11), 5380–5552.
[28] Klimont, Z., Kupiainen, K., Heyes, C., Purohit, P., Cofala, J., Rafaj, P., Borken-Kleefeld, J., Schöpp, W., 2017. Global anthropogenic emissions of particulate matter including black carbon. Atmos. Chem. Phys 17 (14), 8681–8723.
[29] Currie, L.A., Klouda, G.A., Continetti, R.E., Kaplan, I.R., Wong, W.W., Dzubay, T. G., Stevens, R.K., 1983. On the origin of carbonaceous particles in American cities: Results of radiocarbon "Dating" and chemical characterization. Radiocarbon 25, 603–614.
[30] Heal, M.R., Naysmith, P., Cook, G.T., Xu, S., Duran, T.R., Harrison, R.M., 2011. Application of ^{14}C analyses to source apportionment of carbonaceous $PM_{2.5}$ in the UK. Atmos Environ 45 (14), 2341–2348.
[31] Hildemann, L.M., Klinedinst, D.B., Klouda, G.A., Currie, L.A., Cass, G.R., 1994. Sources of urban contemporary carbon aerosol. Environ Sci Technol 28 (9), 1565–1576.
[32] Zhang, Y.-L., Cerqueira, M., Salazar, G., Zotter, P., Hueglin, C., Zellweger, C., Pio, C., Prévôt, A.S.H., Szidat, S., 2015. Wet deposition of fossil and non-fossil derived particulate carbon: Insights from radiocarbon measurement. Atmos Environ 115, 257–262.
[33] Minguillón, M.C., Perron, N., Querol, X., Szidat, S., Fahrni, S.M., Alastuey, A., Jimenez, J.L., Mohr, C., Ortega, A.M., Day, D.A., Lanz, V.A., Wacker, L., Reche, C., Cusack, M., Amato, F., Kiss, G., Hoffer, A., Decesari, S., Moretti, F., Hillamo, R., Teinilä, K., Seco, R., Peñuelas, J., Metzger, A., Schallhart, S., Müller, M., Hansel, A., Burkhart, J.F., Baltensperger, U., Prévôt, A.S.H., 2011. Fossil versus contemporary sources of fine elemental and organic carbonaceous particulate matter during the DAURE campaign in Northeast Spain. Atmos Chem Phys 11 (23), 12067–12084.
[34] Currie, L.A., 2000. Evolution and multidisciplinary frontiers of ^{14}C aerosol science. Radiocarbon 42 (1), 115–126.
[35] Zhang, X., Li, J., Zhu, S., Liu, J., Ding, P., Gao, S., Tian, C., Chen, Y., Peng, P., Zhang, G., 2023. Technical note: Intercomparison study of the elemental carbon radiocarbon analysis methods using synthetic known samples. Atmos Chem Phys 23 (13), 7495–7502.
[36] Ascough, P.L., Bird, M.I., Brock, F., Higham, T.F.G., Meredith, W., Snape, C.E., Vane, C.H., 2009. Hydropyrolysis as a new tool for radiocarbon pre-treatment and the quantification of black carbon. Quat Geochronol 4 (2), 140–147.
[37] Ascough, P.L., Bird, M.I., Meredith, W., Wood, R.E., Snape, C.E., Brock, F., Higham, T.F.G., Large, D.J., Apperley, D.C., 2010. Hydropyrolysis: Implications for radiocarbon pretreatment and characterization of black carbon. Radiocarbon 52 (3), 1336–1350.
[38] Zhang, X., Li, J., Mo, Y., Shen, C., Ding, P., Wang, N., Zhu, S., Cheng, Z., He, J., Tian, Y., Gao, S., Zhou, Q., Tian, C., Chen, Y., Zhang, G., 2019. Isolation and radiocarbon analysis of elemental carbon in atmospheric aerosols using hydropyrolysis. Atmos Environ 198, 381–386.
[39] Meredith, W., Ascough, P.L., Bird, M.I., Large, D.J., Snape, C.E., Sun, Y., Tilston, E. L., 2012. Assessment of hydropyrolysis as a method for the quantification of black carbon using standard reference materials. Geochim Cosmochim Ac 97, 131–147.
[40] Ascough, P., Bompard, N., Garnett, M.H., Gulliver, P., Murray, C., Newton, J.A., Taylor, C., 2024. ^{14}C measurement of samples for environmental science applications at the national environmental isotope facility (NEIF) radiocarbon laboratory, SUERC, UK. Radiocarbon 66 (5), 1020–1031.
[41] Reimer, P., Brown, T., Reimer, R., 2004. Discussion: Reporting and calibration of post-bomb ^{14}C data. Radiocarbon 46, 1299–1304.
[42] Gelencsér, A., May, B., Simpson, D., Sánchez-Ochoa, A., Kasper-Giebl, A., Puxbaum, H., Caseiro, A., Pio, C., Legrand, M., 2007. Source apportionment of $PM_{2.5}$ organic aerosol over Europe: Primary/secondary, natural/anthropogenic, and fossil/biogenic origin. J Geophys Res Atmos 112 (D23).
[43] Lewis, C.W., Klouda, G.A., Ellenson, W.D., 2004. Radiocarbon measurement of the biogenic contribution to summertime $PM_{2.5}$ ambient aerosol in Nashville. Tn Atmos Environ 38 (35), 6053–6061.
[44] Palstra, S.W.L., Meijer, H.A.J., 2014. Biogenic carbon fraction of biogas and natural gas fuel mixtures determined with ^{14}C. Radiocarbon 56 (1), 7–28.
[45] Zhang, Y., Ren, H., Sun, Y., Cao, F., Chang, Y., Liu, S., Lee, X., Agrios, K.A., Kawamura, K., Liu, D., Ren, L., Du, W., Wang, Z., Prévôt, A.S.H., Szidat, S., Fu, P., 2017. High contribution of nonfossil sources to submicrometer organic aerosols in Beijing, China. Environ Sci Technol 51 (14), 7842–7852.
[46] Zhang, Y.L., Zotter, P., Perron, N., Prévôt, A.S.H., Wacker, L., Szidat, S., 2013. Fossil and non-fossil sources of different carbonaceous fractions in fine and coarse particles by radiocarbon measurement. Radiocarbon 55 (3), 1510–1520.
[47] Levin, I., Naegler, T., Kromer, B., Diehl, M., Francey, R.J., Gomez-Pelaez, A.J., Steele, L.P., Wagenbach, D., Weller, R., Worthy, D.E., 2010. Observations and modelling of the global distribution and long-term trend of atmospheric $^{14}CO_2$. Tellus B. https://doi.org/10.1111/j.1600-0889.2009.00446.x.
[48] Hou, S., Liu, D., Xu, J., Vu, T.V., Wu, X., Srivastava, D., Fu, P., Li, L., Sun, Y., Vlachou, A., Moschos, V., Salazar, G., Szidat, S., Prévôt, A.S.H., Harrison, R.M., Shi, Z., 2021. Source apportionment of carbonaceous aerosols in Beijing with radiocarbon and organic tracers: Insight into the differences between urban and rural sites. Atmos Chem Phys 21 (10), 8273–8292.
[49] Shukla, A.K., Tripathi, S.N., Talukdar, S., Murari, V., Gaddamidi, S., Manousakas, M.I., Lalchandani, V., Dixit, K., Ruge, V.M., Khare, P., Kumar, M., Singh, V., Rastogi, N., Tiwari, S., Srivastava, A.K., Ganguly, D., Daellenbach, K.R., Prévôt, A.S.H., 2025. Measurement report: Sources and meteorology influencing highly time-resolved $PM_{2.5}$ trace elements at three urban sites in the extremely polluted Indo-Gangetic Plain in India. Atmos Chem Phys 25 (6), 3765–3784.
[50] Velásquez-García, M.P., Hernández, K.S., Vergara-Correa, J.A., Pope, R.J., Gómez-Marín, M., Rendón, A.M., 2024. Long-range transport of air pollutants increases the concentration of hazardous components of $PM_{2.5}$ in northern South America. Atmos Chem Phys 24 (20), 11497–11520.
[51] Vispute, A.S., Acharja, P., Gosavi, S.W., Govardhan, G., Ruge, V., Patil, M.N., Dharmaraj, T., Ghude, S.D., 2025. Source characteristics of non-refractory particulate matter (NR-PM_1) using high-resolution time-of-flight aerosol mass spectrometric (HR-ToF-AMS) measurements in the urban industrial city in India. Atmos Environ 351, 121186.
[52] Zhang, D., Huang, X., Xiao, S., Zhang, Z., Zhang, Y., Wang, X., 2024. Characterization and sources of VOCs during $PM_{2.5}$ pollution periods in a typical city of the Yangtze River Delta. Atmosphere 15 (10), 1162.
[53] Cash, J.M., Langford, B., Di Marco, C., Mullinger, N.J., Allan, J., Reyes-Villegas, E., Joshi, R., Heal, M.R., Acton, W.J.F., Hewitt, C.N., Misztal, P.K., Drysdale, W., Mandal, T.K., Shivani, Gadi, R., Gurjar, B.R., Nemitz, E., 2021. Seasonal analysis of submicron aerosol in Old Delhi using high-resolution aerosol mass spectrometry: chemical characterisation, source apportionment and new marker identification. Atmos Chem Phys 21 (13), 10133–10158.
[54] Reyes-Villegas, E., Panda, U., Darbyshire, E., Cash, J.M., Joshi, R., Langford, B., Di Marco, C.F., Mullinger, N.J., Alam, M.S., Crilley, L.R., Rooney, D.J., Acton, W.J.F., Drysdale, W., Nemitz, E., Flynn, M., Voliotis, A., McFiggans, G., Coe, H., Lee, J., Hewitt, C.N., Heal, M.R., Gunthe, S.S., Mandal, T.K., Gurjar, B.R., Shivani, Gadi, R., Singh, S., Soni, V., Allan, J.D., 2021. PM_1 composition and source apportionment at two sites in Delhi, India, across multiple seasons. Atmos Chem Phys 21 (15), 11655–11667.
[55] Bank, W., 2023. Manuf Value added.

[56] Huang, R.-J., Zhang, Y., Bozzetti, C., Ho, K.-F., Cao, J.-J., Han, Y., Daellenbach, K. R., Slowik, J.G., Platt, S.M., Canonaco, F., Zotter, P., Wolf, R., Pieber, S.M., Bruns, E.A., Crippa, M., Ciarelli, G., Piazzalunga, A., Schwikowski, M., Abbaszade, G., Schnelle-Kreis, J., Zimmermann, R., An, Z., Szidat, S., Baltensperger, U., Haddad, I.E., Prévôt, A.S.H., 2014. High secondary aerosol contribution to particulate pollution during haze events in China. Nature 514 (7521), 218–222.
[57] Zhang, Y.L., Huang, R.J., El Haddad, I., Ho, K.F., Cao, J.J., Han, Y., Zotter, P., Bozzetti, C., Daellenbach, K.R., Canonaco, F., Slowik, J.G., Salazar, G., Schwikowski, M., Schnelle-Kreis, J., Abbaszade, G., Zimmermann, R., Baltensperger, U., Prévôt, A.S.H., Szidat, S., 2015. Fossil vs. non-fossil sources of fine carbonaceous aerosols in four Chinese cities during the extreme winter haze episode of 2013. Atmos Chem Phys 15 (3), 1299–1312.
[58] Zhang, Y.L., Kawamura, K., Agrios, K., Lee, M., Salazar, G., Szidat, S., 2016. Fossil and nonfossil sources of organic and elemental carbon aerosols in the outflow from northeast China. Environ Sci Technol 50 (12), 6284–6292.
[59] Agarwal, S., Mandal, P., Majumdar, D., Aggarwal, S.G., Srivastava, A., 2016. Characterization of bioaerosols and their relation with OC, EC and carbonyl VOCs at a busy roadside restaurants-cluster in New Delhi. Aerosol Air Qual Res 16 (12), 3198–3211.
[60] Crippa, M., Canonaco, F., Lanz, V.A., Äijälä, M., Allan, J.D., Carbone, S., Capes, G., Ceburnis, D., Dall'Osto, M., Day, D.A., DeCarlo, P.F., Ehn, M., Eriksson, A., Freney, E., Hildebrandt Ruiz, L., Hillamo, R., Jimenez, J.L., Junninen, H., Kiendler-Scharr, A., Kortelainen, A.M., Kulmala, M., Laaksonen, A., Mensah, A.A., Mohr, C., Nemitz, E., O'Dowd, C., Ovadnevaite, J., Pandis, S.N., Petäjä, T., Poulain, L., Saarikoski, S., Sellegri, K., Swietlicki, E., Tiitta, P., Worsnop, D.R., Baltensperger, U., Prévôt, A.S.H., 2014. Organic aerosol components derived from 25 AMS data sets across Europe using a consistent ME-2 based source apportionment approach. Atmos Chem Phys 14 (12), 6159–6176.
[61] Mohr, C., Huffman, J.A., Cubison, M.J., Aiken, A.C., Docherty, K.S., Kimmel, J.R., Ulbrich, I.M., Hannigan, M., Jimenez, J.L., 2009. Characterization of primary organic aerosol emissions from meat cooking, trash burning, and motor vehicles with high-resolution aerosol mass spectrometry and comparison with ambient and chamber observations. Environ Sci Technol 43 (7), 2443–2449.
[62] Xu, L., Suresh, S., Guo, H., Weber, R.J., Ng, N.L., 2015. Aerosol characterization over the southeastern United States using high-resolution aerosol mass spectrometry: Spatial and seasonal variation of aerosol composition and sources with a focus on organic nitrates. Atmos Chem Phys 15 (13), 7307–7336.
[63] Hopke, P.K., 2016. Review of receptor modeling methods for source apportionment. J Air Waste Manag Assoc 66 (3), 237–259.
[64] Shi, G., Xu, J., Peng, X., Tian, Y., Wang, W., Han, B., Zhang, Y., Feng, Y., Russell, A. G., 2016. Using a new WALSPMF model to quantify the source contributions to $PM_{2.5}$ at a harbour site in China. Atmos Environ 126, 66–75.
[65] Stuiver, M., Polach, H.A., 1977. Discussion: Reporting of ^{14}C Data. Radiocarbon 19, 355–363.
[66] Zhang, X., Li, J., Zhu, S., Liu, J., Ding, P., Gao, S., Tian, C., Chen, Y., Peng, P., Zhang, G., 2023. Technical note: Intercomparison study of the EC radiocarbon analysis methods using synthetic known samples. EGUsphere 2023, 1–13.
[67] Zotter, P., Ciobanu, V.G., Zhang, Y.L., El-Haddad, I., Macchia, M., Daellenbach, K. R., Salazar, G.A., Huang, R.J., Wacker, L., Hueglin, C., Piazzalunga, A., Fermo, P., Schwikowski, M., Baltensperger, U., Szidat, S., Prévôt, A.S.H., 2014. Radiocarbon analysis of elemental and organic carbon in Switzerland during winter-smog episodes from 2008 to 2012 – Part 1: Source apportionment and spatial variability. Atmos Chem Phys 14 (24), 13551–13570.
[68] Takegawa, N., Miyazaki, Y., Kondo, Y., Komazaki, Y., Miyakawa, T., Jimenez, J.L., Jayne, J.T., Worsnop, D.R., Allan, J.D., Weber, R.J., 2005. Characterization of an aerodyne aerosol mass spectrometer (AMS): Intercomparison with other aerosol instruments. Aerosol Sci Technol 39 (8), 760–770.
[69] Paatero, P., 1997. Least squares formulation of robust non-negative factor analysis. Chemom Intell Lab 37 (1), 23–35.
[70] Xu, J., Srivastava, D., Wu, X., Hou, S., Vu, T.V., Liu, D., Sun, Y., Vlachou, A., Moschos, V., Salazar, G., Szidat, S., Prévôt, A.S.H., Fu, P., Harrison, R.M., Shi, Z., 2021. An evaluation of source apportionment of fine OC and $PM_{2.5}$ by multiple methods: APHH-Beijing campaigns as a case study. Faraday Discuss 226 (0), 290–313.
[71] Bhattu, D., Tripathi, S.N., Bhowmik, H.S., Moschos, V., Lee, C.P., Rauber, M., Salazar, G., Abbaszade, G., Cui, T., Slowik, J.G., Vats, P., Mishra, S., Lalchandani, V., Satish, R., Rai, P., Casotto, R., Tobler, A., Kumar, V., Hao, Y., Qi, L., Khare, P., Manousakas, M.I., Wang, Q., Han, Y., Tian, J., Darfeuil, S., Minguillon, M.C., Hueglin, C., Conil, S., Rastogi, N., Srivastava, A.K., Ganguly, D., Bjelic, S., Canonaco, F., Schnelle-Kreis, J., Dominutti, P.A., Jaffrezo, J.-L., Szidat, S., Chen, Y., Cao, J., Baltensperger, U., Uzu, G., Daellenbach, K.R., El Haddad, I., Prévôt, A.S.H., 2024. Local incomplete combustion emissions define the $PM_{2.5}$ oxidative potential in Northern India. Nat Commun 15 (1), 3517.
[72] Evangelista, H., Maldonado, J., Godoi, R.H.M., Pereira, E.B., Koch, D., Tanizaki-Fonseca, K., Van Grieken, R., Sampaio, M., Setzer, A., Alencar, A., Gonçalves, S.C., 2007. Sources and transport of urban and biomass burning aerosol black carbon at the South–West Atlantic Coast. J Atmos Chem 56 (3), 225–238.
[73] Geng, X., Haig, J., Lin, B., Tian, C., Zhu, S., Cheng, Z., Yuan, Y., Zhang, Y., Liu, J., Zheng, M., Li, J., Zhong, G., Zhao, S., Bird, M.I., Zhang, G., 2023. Provenance of aerosol black carbon over northeast Indian Ocean and South China Sea and implications for Oceanic black carbon cycling. Environ Sci Technol 57 (35), 13067–13078.
[74] Yang, F., Kawamura, K., Chen, J., Ho, K., Lee, S., Gao, Y., Cui, L., Wang, T., Fu, P., 2016. Anthropogenic and biogenic organic compounds in summertime fine aerosols ($PM_{2.5}$) in Beijing, China. Atmos Environ 124, 166–175.
[75] Jandacka, D., Durcanska, D., Bujdos, M., 2017. The contribution of road traffic to particulate matter and metals in air pollution in the vicinity of an urban road. Transp Res DTr E 50, 397–408.
[76] Mogno, C., Palmer, P.I., Marvin, M.R., Sharma, S., Chen, Y., Wild, O., 2023. Road transport impact on $PM_{2.5}$ pollution over Delhi during the post-monsoon season. Atmos. Environ 17, 100200.
[77] Wei, N., Xu, Z., Wang, G., Liu, W., Zhouga, D., Xiao, D., Yao, J., 2019. Source apportionment of carbonaceous aerosols during haze days in Shanghai based on dual carbon isotopes. J Radioanal Nucl Chem 321 (2), 383–389.
[78] Harrison, R.M., 2020. Airborne particulate matter. Philos T R Soc A 378 (2183), 20190319.
[79] Singh, A.K., Srivastava, A., 2021. Seasonal trends of organic and elemental carbon in PM_1 measured over an industrial area of Delhi, India. Aerosol Sci Technol 5 (1), 112–125.
[80] Watson, J.G., Chow, J.C., Lowenthal, D.H., Pritchett, L.C., Frazier, C.A., Neuroth, G.R., Robbins, R., 1994. Differences in the carbon composition of source profiles for diesel- and gasoline-powered vehicles. Atmos Environ 28 (15), 2493–2505.
[81] Shi, J.P., Mark, D., Harrison, R.M., 2000. Characterization of particles from a current technology heavy-duty diesel engine. Environ Sci Technol 34 (5), 748–755.
[82] Kamat, D.K., Sharma, S.K., Kumar, P., Kumar, K.N., Saha, S., Kaur, Aniket, S., Arun, 2026. Atmospheric boundary layer characteristics during severe air pollution and fog events over Delhi: Insights from ground-based Lidar, satellites, and models. Atmos Environ 367, 121684.
[83] Murthy, B.S., Latha, R., Tiwari, A., Rathod, A., Singh, S., Beig, G., 2020. Impact of mixing layer height on air quality in winter. J Atmos SolTerr Phys 197, 105157.
[84] Sharma, P., Peshin, S.K., Soni, V.K., Singh, S., Beig, G., Ghosh, C., 2022. Seasonal dynamics of particulate matter pollution and its dispersion in the city of Delhi, India. Meteorol Atmos Phys 134 (2), 28.
[85] Bikkina, S., Andersson, A., Ram, K., Sarin, M.M., Sheesley, R.J., Kirillova, E.N., Rengarajan, R., Sudheer, A.K., Gustafsson, Ö., 2017. Carbon isotope-constrained seasonality of carbonaceous aerosol sources from an urban location (Kanpur) in the Indo-Gangetic Plain. J Geophys Res Atmos 122 (9), 4903–4923.
[86] Dasari, S., Andersson, A., Stohl, A., Evangeliou, N., Bikkina, S., Holmstrand, H., Budhavant, K., Salam, A., Gustafsson, Ö., 2020. Source quantification of South Asian black carbon aerosols with isotopes and modeling. Environ Sci Technol 54 (19), 11771–11779.
[87] Kaskaoutis, D.G., Kumar, S., Sharma, D., Singh, R.P., Kharol, S.K., Sharma, M., Singh, A.K., Singh, S., Singh, A., Singh, D., 2014. Effects of crop residue burning on aerosol properties, plume characteristics, and long-range transport over northern India. J Geophys Res 119 (9), 5424–5444.
[88] Paul, D., Singh, G.K., Gupta, T., Chatterjee, A., Saikia, B.K., Sunder Raman, R., Habib, G., Phuleria, H., Venkataraman, C., 2025. Assessment of stable carbon isotope ratios and source characterization of aerosols in ambient $PM_{2.5}$ from the Indian COALESCE network. Sci Rep 15 (1), 19503.
[89] Singh, G., Choudhary, V., Gupta, T., Paul, D., 2019. Investigation of size distribution and mass characteristics of ambient aerosols and their combustion sources during post-monsoon in Northern India. Atmos Pollut Res 11.
[90] Singh, G., Rajeev, P., Paul, D., Gupta, T., 2022. Insights into sources and atmospheric processing at two polluted urban locations in the Indo-Gangetic plains from stable carbon and nitrogen isotope ratios and polycyclic aromatic hydrocarbons in ambient $PM_{2.5}$. Atmos Environ 271, 118904.
[91] Singh, G.K., Choudhary, V., Rajeev, P., Paul, D., Gupta, T., 2021. Understanding the origin of carbonaceous aerosols during periods of extensive biomass burning in northern India. Environ Pollut 270, 116082.
[92] Gustafsson, Ö., Kruså, M., Zencak, Z., Sheesley, R.J., Granat, L., Engström, E., Praveen, P.S., Rao, P.S.P., Leck, C., Rodhe, H., 2009. Brown clouds over South Asia: Biomass or fossil fuel combustion? Science 323 (5913), 495–498.
[93] Nagar, P.K., Singh, D., Sharma, M., Kumar, A., Aneja, V.P., George, M.P., Agarwal, N., Shukla, S.P., 2017. Characterization of $PM_{2.5}$ in Delhi: Role and impact of secondary aerosol, burning of biomass, and municipal solid waste and crustal matter. Environ Sci Pollut Res Int 24 (32), 25179–25189.
[94] Sawlani, R., Agnihotri, R., Sharma, C., Patra, P.K., Dimri, A.P., Ram, K., Verma, R. L., 2019. The severe Delhi SMOG of 2016: A case of delayed crop residue burning, coincident firecracker emissions, and atypical meteorology. Atmos Pollut Res 10 (3), 868–879.
[95] Ndah, F., Valolahti, H., Schollert, M., Michelsen, A., Rinnan, R., Kivimäenpää, M., 2022. Influence of increased nutrient availability on biogenic volatile organic compound (BVOC) emissions and leaf anatomy of subarctic dwarf shrubs under climate warming and increased cloudiness. Ann Bot 129 (4), 443–455.
[96] He, Q., Guo, W., Zhang, G., Yan, Y., Chen, L., 2015. Characteristics and seasonal variations of carbonaceous species in $PM_{2.5}$ in Taiyuan, China. Atmosphere 6 (6), 850–862.
[97] Jiang, H., Li, J., Chen, D., Tang, J., Cheng, Z., Mo, Y., Su, T., Tian, C., Jiang, B., Liao, Y., Zhang, G., 2020. Biomass burning organic aerosols significantly influence the light absorption properties of polarity-dependent organic compounds in the Pearl River Delta Region, China. Environ Int 144, 106079.
[98] Srinivas, B., Sarin, M.M., 2014. PM2.5, EC and OC in atmospheric outflow from the Indo-Gangetic Plain: Temporal variability and aerosol organic carbon-to-organic mass conversion factor. Sci Total Environ 487, 196–205.